



In Silico and Multivariate Analysis of Herbal Compounds in Asthma Inflammation: Exploring Alternatives to Corticosteroids

Ayu K. A. Gunawan¹, Putu S. Yustiantara¹, Pande M. N. A. Sari¹, Dyah K. Wati², Masteria Y. Putra³, I M. A. G. Wirasuta^{1*},

¹Department of Pharmacy, Faculty of Mathematics and Natural Sciences, Udayana University, Badung, Bali, Indonesia

²Pediatric Consultant, Critical Care Medicine Udayana University, Sanglah Hospital, Denpasar, Indonesia

³Research Center for Vaccine and Drug, National Research and Innovation Agency (BRIN), Cibinong, West Java, Indonesia

ARTICLE INFO

Article history:

Received 31 December 2024

Revised 24 January 2025

Accepted 31 January 2025

Published online 01 March 2025

Copyright: © 2025 Gunawan *et al.* This is an open-access article distributed under the terms of the [Creative Commons Attribution License](https://creativecommons.org/licenses/by/4.0/), which permits unrestricted use, distribution, and reproduction in any medium, provided the original author and source are credited.

ABSTRACT

Corticosteroids are among the most common therapies for asthma-controlled treatment but, due to their side effects, alternative therapies are being developed. This *in silico* study intends to identify the distinct anti-asthma inflammatory activity of corticosteroids (budesonide and prednisolone) to herbal compounds (cannabidiol, andrographolide, and eucalyptol) toward GR, CB1R, CB2R, TNF- α , IL-1 β , and TGF β 1 targets. *In silico* studies were carried out using PLANTS and AutoDock software. Additional software such as YASARA, MarvinSketch, BIOVIA Discovery Studio Visualizer, and PyMol were used for docking preparation and visualization. RStudio was used to perform multivariate analysis of binding affinity values. ADME characteristics were predicted using pkCSM. Both docking applications identified the TNF- α -eucalyptol interaction as the weakest binding affinity and the CB2-reference exhibited the strongest. The highest binding scores in PLANTS and AutoDock were -133.38 and -13.75 kcal/mol, respectively, while the lowest were -48.12 and -4.19 kcal/mol. Budesonide and prednisolone's binding activities were closest to cannabidiol and andrographolide (similarity>73%). In comparison to other chemicals, eucalyptol has demonstrated the most distinct affinity to the targets (similarity<50%). From all the ligands' ADME characteristics, prednisolone potentially offers the most comprehensive benefits in asthma inflammation treatment, although with higher risk of side effects than budesonide. On the other hand, the herbal compounds demonstrate profiles suitable for systemic therapy, with differences in distribution and clearance that influence their action and side effects. In conclusion, the herbal compounds could be alternative therapies to budesonide and prednisolone in asthma. However, eucalyptol predictably has lower activity.

Keywords: Andrographolide, Asthma inflammation, Budesonide, Corticosteroids, Eucalyptol, *In-silico*, Multivariate analysis, Prednisolone

Introduction

Over the past 30 years, the prevalence of asthma cases globally has risen from 226.9 to 262.41 million and deaths are estimated to be 461.07 thousand.¹ Asthma is characterized by airway inflammation causing symptoms such as wheezing, shortness of breath, chest tightness, and coughing.^{2,3} Historically, asthma is classified into two forms: allergic, triggered by dust, pollen, and animal dander, for example and non-allergic, triggered by glycolipids, pollutants, and microbes.³ Once the triggers enter the body, an immune response is produced, leading to inflammation and airway remodeling. Asthma's immune response is initiated by activating immune cells. This initial response releases pro-inflammatory cytokines, including tumor necrosis factors- α (TNF- α) and interleukin-1beta (IL-1 β), by mast cells, macrophages, and dendritic cells to prevent further asthma exacerbation.

*Corresponding author. E mail: mgelgell@yahoo.de

Tel: +62 813-3774-2733

Citation: Gunawan AK, Yustiantara PS, Sari PM, Wati DK, Putra MY,³ I M. A. G. Wirasuta IM. In Silico and Multivariate Analysis of Herbal Compounds in Asthma Inflammation: Exploring Alternatives to Corticosteroids. Trop J Nat Prod Res. 2025; 9(2): 817 – 825 <https://doi.org/10.26538/tjnpr/v9i2.51>

Official Journal of Natural Product Research Group, Faculty of Pharmacy, University of Benin, Benin City, Nigeria

These cytokines are essential in recruiting eosinophils and neutrophils to the airways, promoting inflammatory response.^{4,5} As the asthma inflammation persists, TGF- β through TGF- β receptor one kinase (TGF β 1) will mediate airway remodeling by modulating fibroblast proliferation and collagen deposition, causing the airway wall to thicken.⁶ In a parallel way, part of the endocannabinoid system, the cannabinoid 1 (CB1) and CB2 receptors, contribute to neuromodulators' immune response through neural pathways.^{7,8} The pro-inflammatory cytokines and endocannabinoid system's targets are interconnected in the immune response of asthma inflammation (Figure 1).

Inhaled corticosteroids (ICS) like budesonide are the mainstay of long-term asthma control treatment. In some cases, oral corticosteroids (OCs), such as prednisolone are needed to manage acute exacerbations.⁹ Glucocorticoid receptor (GR) is targeted by corticosteroids to reduce inflammation by activating anti-inflammatory genes and suppressing pro-inflammatory genes.¹⁰ However, prolonged use of corticosteroids can cause side effects, such as osteoporosis, immunosuppression, and weight gain.¹¹ These side effects are related to the interaction of drug compounds with molecular targets (Table 1). This issue highlights the need for alternative therapies. In this context, cannabidiol, andrographolide, and eucalyptol compounds that have shown promising results in managing asthma-related inflammation.^{8,11-14}

To investigate alternative therapies to manage asthma exacerbation, *in silico* methods have become invaluable tools for evaluating potential compounds, offering rapid, effective, and economical tool for

development of new drugs.¹⁵ PLANTS and AutoDock were used in the silico analysis to simulate the binding affinities and interactions between compounds and key targets involved in asthma inflammation. To further analyze the molecular docking results, multivariate analysis was applied to uncover deeper data patterns and simplify complex datasets. Principal component analysis (PCA) and hierarchical cluster analysis (HCA) were used to provide different perspectives. PCA simplified the multivariate data by reducing its dimensions based on its principal components (PCs). PCs maintain the most significant degree

of variance from the data collection and are orthogonal to each other.¹⁶ On the other hand, HCA provides a mechanism to classify the data based on similarity. By integrating a dual docking method and multivariate analysis, this study aims to compare the effectiveness and potential side effects of conventional drugs (budesonide and prednisolone) and herbal compounds (cannabidiol, andrographolide, and eucalyptol) based on their binding activity through targeted receptors that involved in asthma inflammation.

Table 1: Molecular Docking's Key Targets

Target	Contribution in Asthma Inflammation	Potential Side Effect Involves
Glucocorticoid Receptor (GR)	Activate anti-inflammatory genes and suppress pro-inflammatory genes. ¹⁰	Osteoporosis, immunosuppression, and weight gain. ⁵²⁻⁵⁴
Cannabinoid 1 receptor (CB1R)	Potentially promotes the release of pro-inflammatory mediators ⁸	Osteoporosis, weight gain. ^{55,56}
Cannabinoid 2 receptor (CB2R)	Regulates the activation of ILC2s (innate lymphoid cells), key players in airway inflammation ⁷	Immunosuppression. ⁵⁷
Tumor Necrosis Factor-Alpha (TNF- α)	Modulator of pro-inflammatory cytokines release, activate eosinophils and neutrophils. ⁵	Osteoporosis, immunosuppression, weight gain. ⁵⁸⁻⁶⁰
Interleukin-1 Beta (IL-1 β)	Initiating release of other pro-inflammatory factors, promoting eosinophils and neutrophils. ⁶¹	Osteoporosis, immunosuppression. ^{62,63}
Transforming Growth Factor-Beta Receptor 1 kinase (TGFB β 1)	Modulates fibroblast proliferation and collagen deposition, according to differentiation in airways. ⁶	Osteoporosis, immunosuppression. ^{64,65}

Materials and Methods

Molecular Docking

Proteins Preparation

The 3D structures of the targets were obtained from a protein data bank (<https://www.rcsb.org>) with the PDB IDs 6EL9 (GR), 5U09 (CB1R), 6KPC (CB2R), 6X81 (TNF- α), 8C3U (IL-1 β), and 1PY5 (TGFB β 1). Different protein formats were needed to simulate molecular docking tests using the Protein-Ligand ANT System (PLANTS) and AutoDock 4.2.6, along with AutoDock Tools 1.5.6. In the PLANTS simulation, the protein used was in .mol2 format. YASARA version 10.1.8, as an additional software was used to remove unnecessary molecules and to add hydrogen atoms, leaving only the selected protein chain and its residues in .mol2 file format, which was then used for docking tests.¹⁷ Meanwhile, BIOVIA Discovery Studio Visualizer v.24.1.0.23298 was used to remove water molecules and to select the desired protein chain for AutoDock simulation. The edited structure was saved in .pdb file format. When opening the .pdb file in AutoDock, Kollman charges and polar hydrogens were added and saved in .pqbqt format for further simulation.¹⁸

Ligands Preparation

Ligand compounds cannabidiol, andrographolide, eucalyptol, budesonide, and prednisolone were obtained from PubChem (<https://pubchem.ncbi.nlm.nih.gov>). Ten poses in .mol2 format were required for the PLANTS simulation and created using the MarvinSketch 5.2.5.1 application. Before generating the conformers, the ligand was set to pH 7.4 to match the body's physiological pH.¹⁹ For AutoDock simulation, the 3D molecules downloaded in PubChem were modified in PyMol 2.5.8 to provide the structures in .pdb format. Gasteiger charges for the ligand compound were computed using AutoDock and all hydrogen atoms were added. Non-polar hydrogens were merged and the remaining hydrogen atoms were deleted. At the end of the preparation, the number of torsions was adjusted, and the ligand was saved as a .pdbqt file.^{20,21}

Docking of Protein-Ligand and Docking Visualization

Method validation is key to ensuring the reliability of docking method protocols. The root mean square deviation (RMSD) value between the reference ligand crystallographic pose and the re-docked pose must be less than 2 Å. The PLANTS docking system is based on the ants' colony optimization (ACO) algorithm, which draws inspiration from real ants' ability to obtain the quickest routes between their colony and food supply. PLANTS will provide conformation ranking from docking scores based on piecewise linear potential (PLP) and CHEMPLP scoring function. The scoring function will help to predict a protein's active site based on the most favorable conformer interaction with the binding site.^{22,23} The RMSD of the top conformation docking pose from PLANTS with the reference ligand crystallographic structure was determined using YASARA.

AutoDock 4.2 applies a grid-based method at different locations around the receptor to facilitate effective energy assessments during docking simulation. TNF- α used a 30x30x30 grid box, while the other targets used a 40x40x40 grid box. The grid spacing was set at 0.375 Å. To find the lowest energy configuration, the algorithm identifies conformational space to maximize the interaction of the ligand within the receptor binding site. The scoring function provides the binding free energy as a docking result using a semi-empirical function that blends a Lamarckian genetic algorithm with a free energy force field. To find the optimal ligand conformations, the parameters were set to 100 genetic algorithm (GA) runs and maximum number of evaluations (medium). The Lamarckian genetic algorithm will also considers intermolecular interactions, such as hydrogen bonds, van der Waals forces, and electrostatic interaction binding to determine the binding free energy.^{20,24,25} BIOVIA Discovery Studio Visualizer was used to view the binding interaction of ligand-amino residues.

Multivariate Analysis of Docking Result

Molecular docking binding affinity results were compiled into matrix for analysis using Principal Component Analysis (PCA) and Hierarchical Cluster Analysis (HCA). The PCA results are presented as a biplot that provides a visual overview of each ligand's interaction with the targets. Meanwhile, HCA facilitates the clustering in multivariate data by displaying the relationships between ligands as a

dendrogram. The PCA and HCA analyses were performed using the RStudio 2024.04.2+764 with R 4.4.1.

Pharmacokinetic Predictions

Ligand ADME or pharmacokinetic properties were predicted using the website pkCSM (<https://biosig.lab.uq.edu.au/pkcsm/>)²⁶ and the ligand canonical SMILES were obtained from PubChem.

Results and Discussion

The *in silico* analysis process begins with method validation based on root mean square deviation (RMSD). Other parameters in the *in silico* testing include binding affinity and the interaction of ligands with amino acid residues of the target. The method validation result of the *in silico* study using PLANTS and AutoDock are detailed in Table 2. Based on the RMSD values less than 2 Å, all the methods are valid.²⁷ RMSD values were calculated from the re-docked pose of the ligand to the native binding position within the target.²⁸ A lower RMSD value reflects a ligand pose conformation closer to the native conformation.²⁹ The selected ligand conformation typically features the highest binding affinity towards the target.

Table 2 also shows the binding affinities of proteins and selected ligands using PLANTS and AutoDock. PLANTS's docking score for reference ligand interaction with targets ranges from -83.14 to -133.38, yet AutoDock has lower scores, from -8.80 to -13.75. The 8.7-fold higher scores in PLANTS than AutoDock are due to different scoring units. AutoDock calculates free binding energy (kcal/mol) represented by the predicted binding affinity and it gives insights into the thermodynamics of the interaction.³⁰ Meanwhile, PLANTS does not directly correspond to an energy value but is empirical and focuses on the geometry of the protein-ligand interaction. The score does not have physical units but provides a relative pose ranking based on the binding's quality.³¹ Thus, both docking results are normalized before proceeding with further multivariate analysis. This study normalized the data by expressing each ligand's docking score as a relative percentage of the reference ligand's score.

Figure 2A, 2B, and 2C present principal component analysis (PCA) plots illustrating the distribution of ligands and targets across the four quadrants of the two-dimensional principal components (PC1 and PC2). These principal components capture the overall variability within the dataset, with PCA employed to reduce the dimensionality of docking data and highlight the differences in binding affinities of various protein-ligand interactions. In the PCA plot for PLANTS (Figure 2A), PC1 accounts for 76.82% of the total variance, while PC2 adds an additional 11.20%, resulting in 88.02% of the total variance explained by the first two components. As expected, PC1 captures the greatest variance, followed by PC2, which is orthogonal to PC1 and captures the second-highest variance. Conversely, the first two components of the AutoDock PCA plot demonstrate higher variance, with PC1 accounting for 89.76% and PC2 for 8.06%, bringing the total explained variance to 97.82%. This indicates that, in AutoDock, differences in binding affinities across ligands are more consistently captured, requiring fewer components to explain nearly all the variance. Additionally, the AutoDock's data shows a higher total variance explained compared to the normalized data (figure 2C), where PC1 and PC2 account for 87.5% and 7.09% of the variance, respectively, totaling 94.59%.

Multivariate analysis investigates the similarity in effectiveness of drug compounds by comparing numerical binding affinity results obtained from molecular docking software. PCA graphics explore the potential mechanism by decreasing the dimensions of the interaction complexities, producing variance from the most dominant variable or binding patterns of docking score data.¹⁶ The squared cosine (cos²) values indicate how well each ligand is represented in the PCA model's principal components, based on PLANTS and AutoDock docking methods.^{32,33} The PCA plot's arrow directions provide insights into ligands' influence on target interactions. Cannabidiol and andrographolide exhibit a similar binding affinity pattern to budesonide and prednisolone, particularly towards the TNF-

α , IL-1 β , and TGFBR1 targets. As shown in Figure 2B, these four compounds clustered in the positive PC1 and PC2 quadrants, similar to IL-1 β , suggesting a comparable interaction profile. A deeper look at Figures 2A and 2B, however, shows that prednisolone has a high representation in the PCA variance (Cos²>0.98) and a substantial correlation with IL-1 β . Although budesonide and andrographolide exhibit a similar binding pattern towards TGFBR1 in Figure 2A, budesonide's Cos² value (0.545) indicates that it contributes the least to the PCs. The binding behavior between these four compounds towards IL-1 β and TGFBR1 shows distinct differences, as evidenced by the opposite positions of the targets in the PCA plot. Eucalyptol consistently shows a binding pattern through TGFBR1 as seen in Figures 2A and 2B, where both were positioned in the negative PC1 and PC2 quadrants. Notably, in AutoDock simulations, eucalyptol demonstrates the highest contribution to the variance, with a Cos² value of 0.996. Across all ligands analyzed, their binding patterns appeared to be opposite to those of GR, CB1, and CB2 targets, although the *in silico* results indicate that each compound has a binding affinity above 60% to reference ligands. Nevertheless, budesonide and prednisolone display the closest binding pattern toward GR and CB1 targets (Figure 2F). Therefore, all compounds possess potential binding capability to the targets, which may produce positive or negative effects.

The potential ligand-target mechanisms from the PCA plots are generally aligned with the hierarchical cluster analysis (HCA) findings (Figures 2D, 2E, and 2F). Cannabidiol and andrographolide indicate potential effectiveness close to that of prednisolone, with a similarity level of over 85%. Budesonide also shows similar activity with the sub-cluster of cannabidiol, andrographolide, and prednisolone, with a similarity level exceeding 73%. In contrast, eucalyptol is located far from the other compound clusters, demonstrating the most distinct activity with a less than 50% similarity. The observation is further supported by eucalyptol's binding affinities toward the targets, which do not exceed 80% for reference ligands.

Comparisons from the multivariate analysis were further analyzed by examining the interaction of amino acid residues in the protein-ligand complex (Table 3). Variation in amino acid residue interactions between a ligand and its target considerably impacts its stability, specificity, and binding affinity, which are factors determining its effectiveness.³⁴ Derived from PLANTS and AutoDock molecular docking results, protein-ligand binding affinity scores (as percentages compared to reference ligands), suggest similarities between the reference ligand and conventional drugs in mechanism of treating asthma inflammation. The binding affinity similarity of budesonide and prednisolone exceeds 77% and the interaction of the amino acid residues involved also supports their similarities.

The ligand-protein complex's binding energy is determined by the kinds and quantity of interactions.³⁵ Hydrophobic and hydrogen bond interactions of protein-ligand complex in the protein binding sites impact all binding energy. Both of these interactions can improve the stability of protein-ligand interactions, causing a reduction in binding affinity value.^{36,37} Hydrogen bonds, which are the bonds that join hydrogen atoms in one molecule to other elements (N, O, and F) in other molecules, exhibit the strongest dipole-dipole force.³⁸ Budesonide and prednisolone exhibit a balanced interaction pattern in the glucocorticoid receptor (GR), engaging both hydrophobic and hydrogen bond (H-bond) interactions to residues (Leu563, Leu608, Met604, Met646, Leu563, and Met560). However, budesonide has one more hydrogen bonding with Phe623, like the native ligand, which enhances its compound binding stability. Cannabidiol, in contrast, has a limited number of hydrogen bonding (Leu563), which leads to a less stable binding profile. Compared to cannabidiol, andrographolide exhibits lower stability because it lacks some hydrophilic interactions. Eucalyptol shows the lowest binding affinity influenced by no H-bond interaction with amino acid residues. This pattern most likely emerges for other receptors. Eucalyptol is the compound that has the least similar amino acid interaction compared to conventional drugs, which is related to the HCA cluster.

Table 2: In silico result (PLANTS docking score and AutoDock free energy binding (kcal/mol))

	RMSD (Å)	Reference		Cannabidiol		Andrographolide		Eucalyptol		Budesonide		Prednisolone	
		BA	%To Ref.	BA	%To Ref.	BA	%To Ref.	BA	%To Ref.	BA	%To Ref.	BA	%To Ref.
GR (P)	1.09	-101.44	100	-90.86	89.57	-82.67	81.50	-56.77	55.96	-94.88	93.54	-88.04	86.79
GR (A)	1.87	-11.66	100	-9.41	80.70	-10.04	86.11	-5.72	49.06	-11.96	102.57	-10.37	88.94
CB1 (P)	1.12	-127.80	100	-90.13	70.52	-93.73	73.34	-60.90	47.65	-82.87	64.84	-78.41	61.35
CB1 (A)	0.99	-12.55	100	-10.45	83.27	-11.29	89.96	-6.17	49.16	-10.90	86.85	-11.37	90.60
CB2 (P)	0.59	-133.38	100	-91.44	68.55	-87.76	65.80	-62.02	46.50	-92.36	69.25	-85.26	63.92
CB2 (A)	0.55	-13.75	100	-11.14	81.02	-11.44	83.20	-6.49	47.2	-10.93	79.49	-10.85	78.91
TNF- α (P)	1.89	-67.48	100	-71.37	105.75	-72.33	107.19	-48.12	71.31	-74.08	109.78	-65.03	96.36
TNF- α (A)	0.90	-5.35	100	-5.70	106.54	-6.26	117.01	-4.19	78.32	-6.07	113.46	-6.12	114.39
IL-1 β (P)	0.88	-106.65	100	-78.70	73.79	-74.82	70.16	-55.74	52.27	-71.53	67.07	-70.51	66.11
IL-1 β (A)	0.76	-11.95	100	-7.36	61.59	-8.49	71.04	-6.04	50.54	-7.87	65.86	-7.55	63.18
TGFBR1 (P)	0.32	-83.14	100	-85.60	102.95	-77.62	93.35	-51.96	62.50	-59.06	71.03	-80.76	97.14
TGFBR1 (A)	0.44	-8.80	100	-8.77	99.66	-9.01	102.39	-5.35	60.80	-9.55	108.52	-8.90	101.14

Where P: PLANTS, A: AutoDock, BA: Binding Affinity, Ref.: Reference

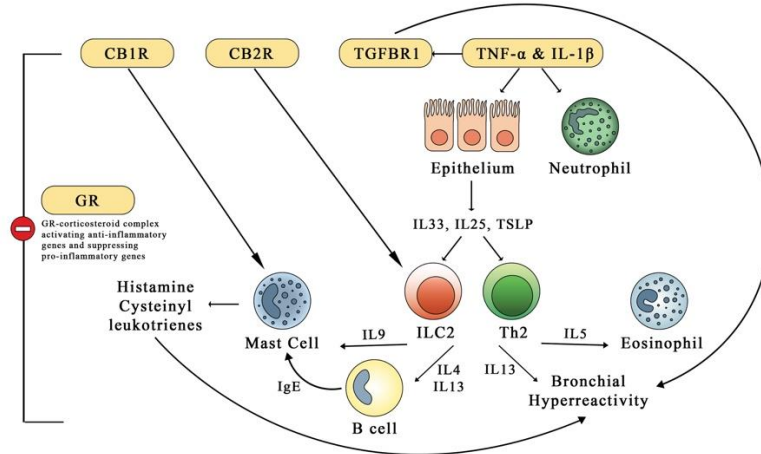


Figure 1: Asthma inflammation relation with selected targets

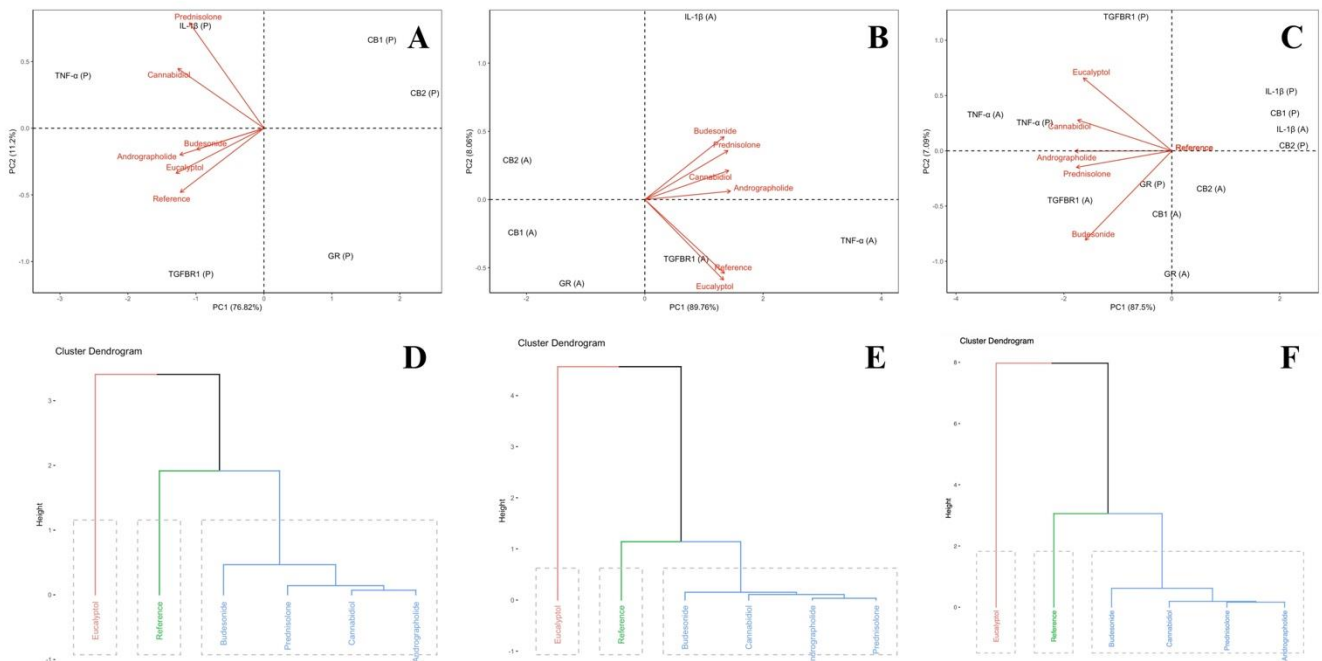


Figure 2: PCA score plot, (A) PLANTS docking score, (B) AutoDock free binding energy, (C) Normalized docking result; HCA of ligands, (D) PLANTS docking score, (E) AutoDock free binding energy, (F) Normalized docking result

Table 3: Amino acid interaction in protein-ligand complex based on AutoDock's molecular docking result

Protein	Ligand	Hydrophobic Interaction	Hydrogen Bond Interaction
GR	Reference	Ala607, Arg611, Cys643, Leu563, Leu566, Leu608, Met560, Met604, Met639, Met646, Phe623	Cys622, Gln570, Leu563, Phe623
	Cannabidiol	Arg611, Leu563, Leu608, Leu753, Met604, Met646, Phe623, Trp600	Leu563
	Andrographolide	Leu566, Leu608, Met601, Met604, Phe623	Leu732, Met604
	Eucalyptol	Leu563, Leu566, Leu608, Met604, Met646, Phe623	-
	Budesonide	Cys643, Leu563, Leu608, Met604, Met639, Met646, Phe623	Asn564, Leu563, Met560, Phe623
CB1R	Prednisolone	Leu608, Phe623, Met646, Leu563, Met604	Leu563, Met560
	Reference	Ala380, Ile105, Leu359, Met103, Met363, Met384, Phe170, Phe268, Trp279, Val196	Ile105, Leu,387, Met103
	Cannabidiol	Ala380, Ile105, Ile169, Phe102, Phe108, Phe189, Phe268, Phe379, Pro269, Val196	Met103
	Andrographolide	Cys386, Met103, Phe268, Phe379, Val196	Ser383
	Eucalyptol	Phe102, Phe108, Phe268, Phe269, Phe379, Met103	Met103
	Budesonide	Met103, Met384, Phe170, Val196	Ile105, Met103, Phe179

CB2R	Prednisolone Reference	Ile105, Met103, Met384, Phe108, Phe170, Phe379 Cys288, His95, Leu191, Met265, Phe117, Phe183, Phe87, Phe91, Phe94, Trp194, Val113, Val261	Pro269, Ser123 His95, Leu182
	Cannabidiol	His95, Ile110, Leu182, Lys278, Phe106, Phe183, Phe91, Phe94, Tyr25, Val113	Pro184
	Andrographolide	His95, Ile110, Lys109, Phe106, Phe183, Phe91, Phe94, Pro184, Val113	His95, Thr114
	Eucalyptol	His95, Phe91, Phe94, Phe183, Pro184, Tyr25, Leu191, Met265, Phe183, Phe87, Phe91, Trp194	- Thr114, Pro184
TNF- α	Budesonide Reference	Phe87, Phe91, Phe183 Gly121, Leu120, Leu57, Tyr59	Pro184, Val113 Ser60, Tyr151
	Cannabidiol	His15, Leu57, Tyr119, Tyr151, Tyr59	Tyr151
	Andrographolide	His15, Leu57, Tyr59, Tyr151	Leu120
	Eucalyptol	Tyr59, Tyr119, Tyr151	-
	Budesonide	Tyr119, Tyr151	-
	Prednisolone Reference	Tyr59, Tyr151 Ala115, Ala59, Lys97, Met95, Pro57, Pro91, Val100, Val3, Val47	Gly121, Tyr119 Asn102, Glu50, Lys93, Lys94, Pro57
	Cannabidiol	Ala59, Lys97, Met95, Pro57, Val100, Val47	Lys94, Met95
IL-1 β	Andrographolide	Ala59, Met95, Pro57, Val3, Val47, Val100	Lys92, Lys97, Ser45
	Eucalyptol	Ala59, Met95, Pro57, Val3, Val47, Val100	-
	Budesonide	Ala115, Lys97, Val47, Val100	Lys94, Phe46, Pro57, Val47
	Prednisolone	Lys94, Lys97, Pro57, Val47, Val100	Lys97, Phe46
	Reference	Ala230, Ile211, Leu260, Leu278, Leu340, Lys232, Val219	Asp281, His283, Ser280, Tyr282
	Cannabidiol	Ala230, Ala350, His283, Ile211, Leu260, Leu278, Leu340, Lys232, Tyr282, Val219	-
	Andrographolide	Ala230, Ile211, Leu340, Val219	His283, Lys337
	Eucalyptol	Ala230, Ala350, Leu260, Leu278, Leu340, Lys232, Tyr249, Val219	-
	Budesonide	Leu340, Ala350, Val219, Leu260, Ala230	Asp290, Ser287
	Prednisolone	Ala230, Ala350, Leu260, Leu340, Val219	Asp290, Gly212, Ile211

Cannabidiol, andrographolide, budesonide, and prednisolone are within the same HCA cluster, indicating that these four compounds have similar potential activity. However, in practice, the side effects observed are distinct. Cannabidiol is reported to have no significant side effects,³⁹ while andrographolide has few mild side effects.⁴⁰ Eucalyptol has the lowest docking score, potentially exhibiting lower effectiveness and side effects on the targets. According to studies, eucalyptol is considered safe when taken in normal dosages.⁴¹ The side effects of each herbal compound will be compared with those of corticosteroids in more detail.

A high binding affinity activity alone does not signify greater therapeutic efficacy and can enhance systemic side effects.^{42,43} For instance, budesonide's binding affinity to its main receptor (GR) is tighter than prednisolone, but this does not necessarily imply that prednisolone has fewer side effects. Budesonide is preferred over prednisolone because the drug is administered directly to the lung, reducing systemic side effects.⁴⁴ Considering these statements, side effects also depend on the drug compound's pharmacokinetic properties (Table 4).

Table 4: ADME (absorption, distribution, metabolism, and excretion) properties affected the potential activity and side effect based on pkCSM

		*1	*2	*3	*4	*5
A	Water solubility (log mol/l)	-4.901	-3.494	-2.63	-4.725	-3.504
	Caco2 permeability (log Papp in 10 ⁻⁶ cm/s)	1.79	1.07	1.485	0.823	0.367
	Intestinal absorption (% Absorbed)	90.657	95.357	96.505	70.994	73.693
D	VDss (log l/kg)	0.939	-0.286	0.491	0.2	-0.198
	BBB (log BB)	-0.113	-0.598	0.368	0.004	-0.503
	CNS (log PS)	-1.886	-2.691	-2.972	-2.882	-3.358
M	CYP3A4 substrate	Yes	Yes	No	Yes	Yes
E	Total clearance (log ml/min/kg)	1.092	1.183	1.009	0.652	0.729

Where *1: Cannabidiol, *2: Andrographolide, *3: Eucalyptol, *4: Budesonide, *5: Prednisolone

In terms of absorption, eucalyptol presents the highest intestinal absorption, followed by andrographolide, cannabidiol, and prednisolone, supporting their effective oral administration by ensuring

good bioavailability in the gastrointestinal tract. Budesonide, with the lowest intestinal absorption, acts locally in the lungs, facilitating targeted respiratory absorption through its moderate Caco2

permeability. Caco2 cells are similar to the human intestinal epithelium, making them the common model to determine the permeability of oral drugs. The predictive value of increased permeability in the Caco2 test is a log Papp value exceeding 0.09.^{45,46} Cannabidiol, andrographolide, and eucalyptol have high Caco2 permeability value ($>1 \times 10^{-6}$ cm/s), demonstrating good cellular penetration and suitability to be administered orally to experience systemic action.⁴⁷ Regarding water solubility, budesonide and cannabidiol are lipophilic and poorly soluble, favoring tissue penetration for local effects in the lungs or deeper systemic effects.⁴⁸ On the other hand, andrographolide, eucalyptol, and prednisolone solubility is slightly greater, which promotes improved systemic circulation.

The highest volume of distribution steady state (VDss) of cannabidiol suggests extensive tissue penetration that may raise the risk of side effects but may possibly be advantageous for systemic therapeutic benefits. Low and high log VDss are <-0.15 and >0.45 , respectively.⁴⁵ Prednisolone's low VDss helps to regulate systemic effects, which is beneficial for treating systemic inflammation predictably, whereas budesonide's moderate VDss is ideal for localized lung activity, limiting systemic exposure. The ligands are also distinguished by their blood-brain barrier (BBB) and central nervous system (CNS) penetration characteristics. A compound will easily pass the blood-brain barrier if the logarithm of blood-brain barrier permeability value (logBB) is greater than 0.3, will be insufficiently distributed if the value of logBB is lower than 0.1, and will be partially dispersed in the brain if the logBB is less than -1.^{45,46} Andrographolide's low BBB and CNS permeability suggests that it may have fewer CNS side effects,⁴⁹ supporting a safer profile for long-term systemic use. The higher BBB permeability value of prednisolone suggests a higher risk of CNS-related adverse effects when taken orally over extended periods of time. Human cytochrome P450 (CYP) enzymes in humans contribute in the metabolism of drugs. More than half of the clinically used medications are metabolised by the CYP3A subfamily, which includes CYP3A4 and has the largest abundance in the liver (~40%) and intestine. CYP3A4 metabolizes all the ligands except eucalyptol, which makes them susceptible to drug-drug interactions if administered with other CYP3A4 substrates or inhibitors.⁵⁰ However, if the drug is administered via inhalation, like budesonide, the systemic metabolism is limited, reducing the chance of such interactions. The clearance rates of cannabidiol and andrographolide are greater, which correlates to faster elimination,⁵¹ making them appropriate for use in shorter therapeutic windows. The low clearance rate of budesonide ensures constant local effects and is useful for prolonged lung retention when inhaled. Although prednisolone usage requires dosing management to avoid accumulation and systemic side effects, its clearance rate aligns with its systemic effects.

Conclusion

Cannabidiol, andrographolide, and eucalyptol have promising potential as therapeutic options for asthma inflammation, substituting budesonide and prednisolone. All the compounds have molecular interactions with asthma inflammation targets, with distinct activities. Notably, eucalyptol has comparatively lower effectiveness and side effects than cannabidiol and andrographolide due to its low affinity to the targets. To validate the activity of these herbal compounds, additional studies are needed to establish their therapeutic efficacy in treating asthma.

Conflict of Interest

The authors declare no conflict of interest.

Authors' Declaration

The authors hereby declare that the work presented in this article are original and that any liability for claims relating to the content of this article will be borne by them.

Acknowledgement

The authors would like to thank the support from Department of Pharmacy, Faculty of Mathematics and Natural Sciences, Udayana University in the process of creating the manuscript.

References

1. Wang Z, Li Y, Gao Y, Fu Y, Lin J, Lei X, Zheng J, Jiang M. Global, regional, and national burden of asthma and its attributable risk factors from 1990 to 2019: a systematic analysis for the Global Burden of Disease Study 2019. *Respir Res.* 2023; 24(1):1–13.
2. Dharmage SC, Perret JL, Custovic A. Epidemiology of Asthma in Children and Adults. *Front Pediatr [Internet].* 2019; 7:1–15.
3. Lambrecht BN, Hammad H. The immunology of asthma. *Nat Immunol.* 2015; 16(1):45–56.
4. Birmann PT, Casaril AM, Zugno GP, Acosta GG, Severo Sabedra Sousa F, Collares T, Seixas FK, Jacob RG, Brüning CA, Savegnago L, Hartwig D. Flower essential oil of *Tagetes minuta* mitigates oxidative stress and restores BDNF-Akt/ERK2 signaling attenuating inflammation- and stress-induced depressive-like behavior in mice. *Brain Res.* 2022;1784:1-12.
5. Mukhopadhyay S, Hoidal JR, Mukherjee TK. Role of TNF α in pulmonary pathophysiology. *Respir Res.* 2006; 7(1):125–133.
6. Kraik K, Tota M, Laska J, Łacwik J, Paździerz Ł, Sędek Ł, Gomułka K. The role of transforming growth factor- β (TGF- β) in asthma and chronic obstructive pulmonary disease (COPD). 2024; 13(15):1271–1293.
7. Palomares O. Could we co-opt the cannabinoid system for asthma therapy? *Expert Rev Clin Immunol.* 2023; 19(10):1183–1186.
8. Vuolo F, Abreu SC, Michels M, Xisto DG, Blanco NG, Hallak JE, Zuardi AW, Crippa JA, Reis C, Bahl M, Pizzichinni E, Maurici R, Pizzichinni MMM, Rocco PRM, Dal-Pizzol F. Cannabidiol reduces airway inflammation and fibrosis in experimental allergic asthma. *Eur J Pharmacol.* 2019; 843:251–259.
9. Global Initiative for Asthma. Global strategy for asthma management and prevention. 2024. Available from: <https://ginasthma.org/2024-report/>
10. Holgate ST, Polosa R. Treatment strategies for allergy and asthma. *Nat Rev Immunol.* 2008; 8(3):218–30.
11. Williams DM. Clinical pharmacology of corticosteroids. *Respir Care.* 2018; 63(6):655–670.
12. Patel SS, Savjani JK. Systematic review of plant steroids as potential antiinflammatory agents: Current status and future perspectives. *J Phytopharm.* 2015; 4(2):121–125.
13. Bao Z, Guan S, Cheng C, Wu S, Wong SH, Kemeny DM, Leung, Bernard P, Wong WSF. A novel antiinflammatory role for andrographolide in asthma via inhibition of the nuclear factor- κ B pathway. *Am J Respir Crit Care Med.* 2009; 179(8):657–665.
14. Juergens LJ, Worth H, Juergens UR. New perspectives for mucolytic, anti-inflammatory and adjunctive therapy with 1,8-Cineole in COPD and asthma: Review on the new therapeutic approach. *Adv Ther.* 2020; 37(5):1737–1753.
15. Galgale S, Zainab R, Kumar A. P, M. N, D. S, Sharma S. Molecular docking and dynamic simulation-based screening identifies inhibitors of targeted SARS-CoV-2 3CLpro and human ACE2. *Int J Appl Pharm.* 2023; 297–308.
16. Granato D, Santos JS, Escher GB, Ferreira BL, Maggio RM. Use of principal component analysis (PCA) and hierarchical cluster analysis (HCA) for multivariate association between bioactive compounds and functional properties in foods: A critical perspective. *Trends Food Sci Technol.* 2018; 72:83–90.
17. Nugroho AA, Hadi MS, Adianto C, Putra JAK, Purnomo H, Fakhruddin N. Molecular docking and ADMET prediction studies of flavonoids as multi-target agents in COVID-19

- therapy: anti-inflammatory and antiviral approaches. *Indones J Pharm.* 2023; 34(4):651–664.
18. Tjitda PJP, Nitbani FO, Parikesit AA, Bessi MIT, Wahyuningsih TD. In silico investigation of tropical natural product for wild-type and quadrupole mutant PfDHFR inhibitors as antimalarial candidates. *Trop J Nat Prod Res.* 2024; 8(2):6208–6217.
 19. Mulyati B, Panjaitan RS. Study of molecular docking of alkaloid derivative compounds from stem karamunting (*Rhodomyrtus tomentosa*) against α -glucosidase enzymes. *Indones J Chem Res.* 2021;9(2):129–136.
 20. Asnawi A, Nedja M, Febrina E, Purwaniati P. Prediction of a stable complex of compounds in the ethanol extract of celery leaves (*Apium graveolens* L.) function as a VKORC1 antagonist. *Trop J Nat Prod Res.* 2023; 7(2):2362–2370.
 21. Nur S, Hanafi M, Setiawan H, Nursamsiar N, Elya B. Molecular docking simulation of reported phytochemical compounds from *Curculigo latifolia* extract on target proteins related to skin antiaging. *Trop J Nat Prod Res.* 2023; 7(11):5067–5080.
 22. Korb O, Stütze T, Exner TE. An ant colony optimization approach to flexible protein–ligand docking. *Swarm Intell.* 2007; 1(2):115–134.
 23. Korb O, Stütze T, Exner TE. Empirical scoring functions for advanced protein–ligand docking with PLANTS. *J Chem Inf Model.* 2009; 49(1):84–96.
 24. Hill AD, Reilly PJ. Scoring functions for autoDock. In: Lütteke T, Frank M, editors. *Glycoinformatics*. New York, NY: Springer New York; 2015. p. 467–474. (Methods in Molecular Biology; vol. 1273).
 25. Morris GM, Huey R, Lindstrom W, Sanner MF, Belew RK, Goodsell DS, Olson AJ. AutoDock4 and AutoDockTools4: Automated docking with selective receptor flexibility. *J Comput Chem.* 2009; 30(16):2785–2791.
 26. Pires DEV, Blundell TL, Ascher DB. pkCSM: Predicting small-molecule pharmacokinetic and toxicity properties using graph-based signatures. *J Med Chem.* 2015; 58(9):4066–4072.
 27. Su M, Yang Q, Du Y, Feng G, Liu Z, Li Y, Wang R. Comparative assessment of scoring functions: The CASF-2016 Update. *J Chem Inf Model.* 2019; 59(2):895–913.
 28. Zheng L, Meng J, Jiang K, Lan H, Wang Z, Lin M, Li W, Guo H, Wei Y, Mu Y. Improving protein–ligand docking and screening accuracies by incorporating a scoring function correction term. *Brief Bioinform.* 2022; 23(3):1–15.
 29. Agistia DD, Purnomo H, Tegar M, Nugroho AE. Interaction between active compounds from *Aegle marmelos* Correa as anti-inflammation agent with COX-1 and COX-2 receptor. *Tradit Med J.* 2013; 18(2):80–87.
 30. Ivanova L, Karelson M. The impact of software used and the type of target protein on molecular docking accuracy. *Molecules.* 2022; 27(24):9041–9060.
 31. Korb O, Stütze T, Exner TE. PLANTS: Application of ant colony optimization to structure-based drug design. In: Dorigo M, Gambardella LM, Birattari M, Martinoli A, Poli R, Stütze T, editors. *Ant colony optimization and swarm intelligence*. Berlin, Heidelberg: Springer Berlin Heidelberg; 2006. p. 247–258.
 32. David CC, Jacobs DJ. Principal Component Analysis: A method for determining the essential dynamics of proteins. In: Livesay DR, editor. *Protein Dynamics*. Totowa, NJ: Humana Press; 2014. p. 193–226.
 33. Ryu J, Liu K, biu, McCloskey TA. The use of multivariate PCA dataset in identifying the underlying drivers of critical stressors, looking at global problems through a local lens. *Data Brief.* 2022;41(2022):1–12.
 34. Febrina E, Alahhari RK, Abdulah R, Lestari K, Levita J, Supratman U. Molecular docking and molecular dynamics studies of *Acalypha indica* L. phytochemical constituents with caspase-3. *Int J Appl Pharm.* 2021;210–215.
 35. Castel B, Tomlinson L, Locci F, Yang Y, Jones JDG. Optimization of T-DNA architecture for Cas9-mediated mutagenesis in Arabidopsis. Lai EM, editor. *PLOS ONE.* 2019;14(1):1–20.
 36. Lisdiana L, Widiatningrum T, Kurniawati F. Original research article molecular docking bioactive compound of rambutan peel (*Nephelium lappaceum* L) and NF-Kb in the context of cigarette smoke-induced inflammation. 2022;6(10):1654–1659.
 37. Inayati I, Arifin NH, Febriansah R, Indarto D, Suryawati B, Hartono H. Trans-Cinnamaldehyde inhibitory activity against mrka, trec, and luxs genes in biofilm-forming *Klebsiella pneumoniae*: An in silico study. *Trop J Nat Prod Res.* 2023; 7(10):4249–4255.
 38. Putra OA, Rahmania TA, Renesteen E. Molecular docking study as therapeutic approach for targeting cholecystokinin in pancreatic cancer. *Int J Appl Pharm.* 2024; 340–349.
 39. Pertwee RG. The diverse CB1 and CB2 receptor pharmacology of three plant cannabinoids: Δ^9 -tetrahydrocannabinol, cannabidiol and Δ^9 -tetrahydrocannabivarin. *Br J Pharmacol.* 2008; 153(2):199–215.
 40. Hidalgo MA, Hancke JL, Bertoglio JC, Burgos RA. Andrographolide a new potential drug for the long term treatment of rheumatoid arthritis disease. In: Matsuno H, editor. *Innovative rheumatology*. InTech; 2013.
 41. Bhowal M, Gopal M. Eucalyptol: Safety and pharmacological profile. *RGUHS J Pharm Sci.* 2016; 5(4):125–131.
 42. Derendorf H, Nave R, Drollmann A, Cerasoli F, Wurst W. Relevance of pharmacokinetics and pharmacodynamics of inhaled corticosteroids to asthma. *Eur Respir J.* 2006; 28(5):1042–1050.
 43. Derendorf H, Hochhaus G, Meibohm B, Möllmann H, Barth J. Pharmacokinetics and pharmacodynamics of inhaled corticosteroids. *J Allergy Clin Immunol.* 1998 ; 101(4):440–446.
 44. Kelly HW. Potential adverse effects of the inhaled corticosteroids. *J Allergy Clin Immunol.* 2003; 112(3):469–478.
 45. Klimoszek D, Jeleń M, Dołowy M, Morak-Młodawska B. Study of the lipophilicity and ADMET parameters of new anticancer diquinothiazines with pharmacophore substituents. *Pharmaceuticals.* 2024; 17(6):725–745.
 46. Rahardhian MRR, Susilawati Y, Musfiroh I, Febriyanti RM, Mughtaridi, Sumiwi SA. In silico study of bioactive compounds from sungkai (*Peronema canescens*) as immunomodulator. *Int J Appl Pharm.* 2022; 135–141.
 47. Artursson P, Karlsson J. Correlation between oral drug absorption in humans and apparent drug permeability coefficients in human intestinal epithelial (Caco-2) cells. *Biochem Biophys Res Commun.* 1991; 175(3):880–885.
 48. Vandamme. Nanocarriers as pulmonary drug delivery systems to treat and to diagnose respiratory and non respiratory diseases. *Int J Nanomedicine.* 2008; 3(1):1–19.
 49. Peterleit AC, Swinney K, Mensch J, Mackie C, Stokbroekx S, Brewster M, Dressman JB. Prediction of blood–brain barrier penetration of poorly soluble drug candidates using surface activity profiling. *Eur J Pharm Biopharm.* 2010; 75(3):405–410.
 50. Zhou SF. Drugs behave as substrates, inhibitors and inducers of human cytochrome P450 3A4. *Curr Drug Metab.* 2008; 9(4):310–322.
 51. Korzekwa K, Nagar S. Process and system clearances in pharmacokinetic models: Our basic clearance concepts are correct. *Drug Metab Dispos.* 2023; 51(4):532–542.
 52. Hsu CH, Hsu CL, Langley A, Wojcik C, Iraganjan E, Grygiel-Górniak B. Glucocorticoid-induced osteoporosis—from molecular mechanism to clinical practice. *Drugs Ther Perspect.* 2024; 40(8):315–329.

53. Meier CA. Mechanisms of immunosuppression by glucocorticoids. *Eur J Endocrinol.* 1996; 134(1):50.
54. Pofi R, Caratti G, Ray DW, Tomlinson JW. Treating the side effects of exogenous glucocorticoids; Can we separate the *good* from the *bad*? *Endocr Rev.* 2023; 44(6):975–1011.
55. O'Sullivan SE, Yates AS, Porter RK. The peripheral cannabinoid receptor type 1 (CB1) as a molecular target for modulating body weight in man. *Molecules.* 2021; 26(20):6178–6192.
56. Wang J, Lu H xia, Wang J. Cannabinoid receptors in osteoporosis and osteoporotic pain: a narrative update of review. *J Pharm Pharmacol.* 2019; 71(10):1469–1474.
57. Basu S, Dittel BN. Unraveling the complexities of cannabinoid receptor 2 (CB2) immune regulation in health and disease. *Immunol Res.* 2011; 51(1):26–38.
58. Evangelatos G, Bamias G, Kitas GD, Kollias G, Sfikakis PP. The second decade of anti-TNF- α therapy in clinical practice: new lessons and future directions in the COVID-19 era. *Rheumatol Int.* 2022; 42(9):1493–1511.
59. Gilbert L, He X, Farmer P, Boden S, Kozlowski M, Rubin J, Nanes MS. Inhibition of osteoblast differentiation by tumor necrosis factor- α *. *Endocrinology.* 2000; 141(11):3956–3964.
60. Patsalos O, Dalton B, Leppanen J, Ibrahim MAA, Himmerich H. Impact of TNF- α inhibitors on body weight and BMI: A systematic review and meta-analysis. *Front Pharmacol.* 2020; 11(481):1–15.
61. Osei ET, Brandsma CA, Timens W, Heijink IH, Hackett TL. Current perspectives on the role of interleukin-1 signalling in the pathogenesis of asthma and COPD. *Eur Respir J.* 2020; 55(2):1–16.
62. De Mooij CEM, Netea MG, Van Der Velden WJFM, Blijlevens NMA. Targeting the interleukin-1 pathway in patients with hematological disorders. *Blood.* 2017; 129(24):3155–3164.
63. Tseng HW, Samuel SG, Schroder K, Lévesque JP, Alexander KA. Inflammasomes and the IL-1 family in bone homeostasis and disease. *Curr Osteoporos Rep.* 2022; 20(3):170–185.
64. Wu M, Chen G, Li YP. TGF- β and BMP signaling in osteoblast, skeletal development, and bone formation, homeostasis and disease. *Bone Res.* 2016; 4(1):1–21.
65. Kim BG, Malek E, Choi SH, Ignatz-Hoover JJ, Driscoll JJ. Novel therapies emerging in oncology to target the TGF- β pathway. *J Hematol Oncol* *J Hematol Oncol.* 2021; 14(1):1–20.